Segmentation of brain tumors using a semi-automatic computational strategy

Segmentation of brain tumors using a semi-automatic computational strategy

M Vera[1,2], Y Huérfano[2], E Gelvez[1], O Valbuena[3], J Salazar[1], V Molina[4], M I Vera[5], W Salazar[5] and F Sáenz[6]

[1] Facultad de Ciencias Básicas y Biomédicas, Universidad Simón Bolívar, San José de Cúcuta, Colombia

[2] Grupo de Investigación en Procesamiento Computacional de Datos, Universidad de Los Andes, Táchira, Venezuela

[3] Grupo de Investigación en Educación Matemática, Matemática y Estadística, Universidad de Pamplona, Pamplona, Colombia

[4] Grupo de investigación GINIC-HUS, Universidad ECCI, Bogotá, Colombia

[5] Servicio de Neurología, Hospital Central, San Cristóbal, Venezuela

[6] Facultad de Ingeniería, Universidad Simón Bolívar, Cúcuta, Colombia

E-mail: m.avera@unisimonbolivar.edu.co

Abstract. In this work, a semi-automatic computational strategy is proposed for brain tumor segmentation. The filtering (erosion + gaussian filters), segmentation (level set technique) and quantification (BT volume) stages are applied to magnetic resonance imaging in order to generate the three-dimensional morphology of brain tumors. The Jaccard's Similarity Index is considered to contrast manual segmentation with semi-automatic segmentations of brain tumor. In this sense, the highest Jaccard's Similarity Index provides the best parameters of the techniques that constitute the semi-automatic computational strategy. Results are promising, showing an excellent correlation between these segmentations. The volume is used for the brain tumors characterization.

1. Introduction

In this paper, brain tumors (BT) are classified according to the American Brain Tumor Association. In this sense, a scheme about the types of BT is presented in Figure 1 [1].

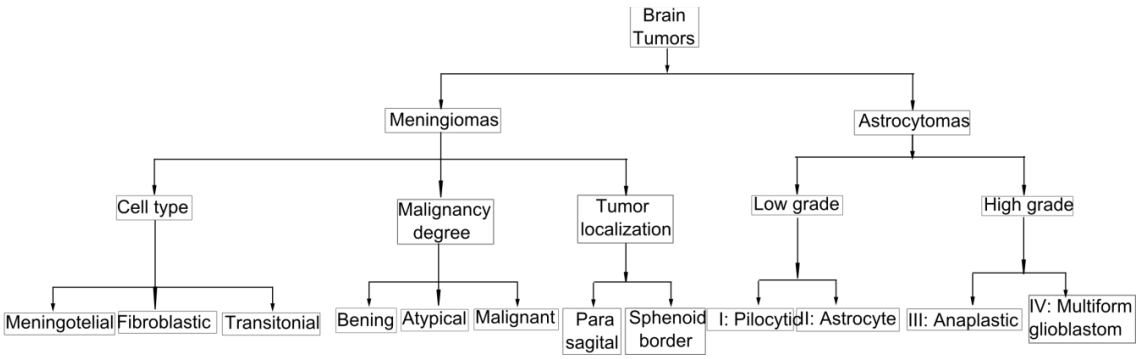

Figure 1. General diagram for BT classification.

Additionally, in the context of digital image processing, the main problem with brain MRI is the Riccian noise [2,3]. In order to approach this problem, usually, a filtering stage is used for modifying the attributes of the images acquired by any of the imaging modalities presented through Figure 2. Although there are different modalities of medical imaging, in this investigation, we chose to work with magnetic resonance imaging (MRI).

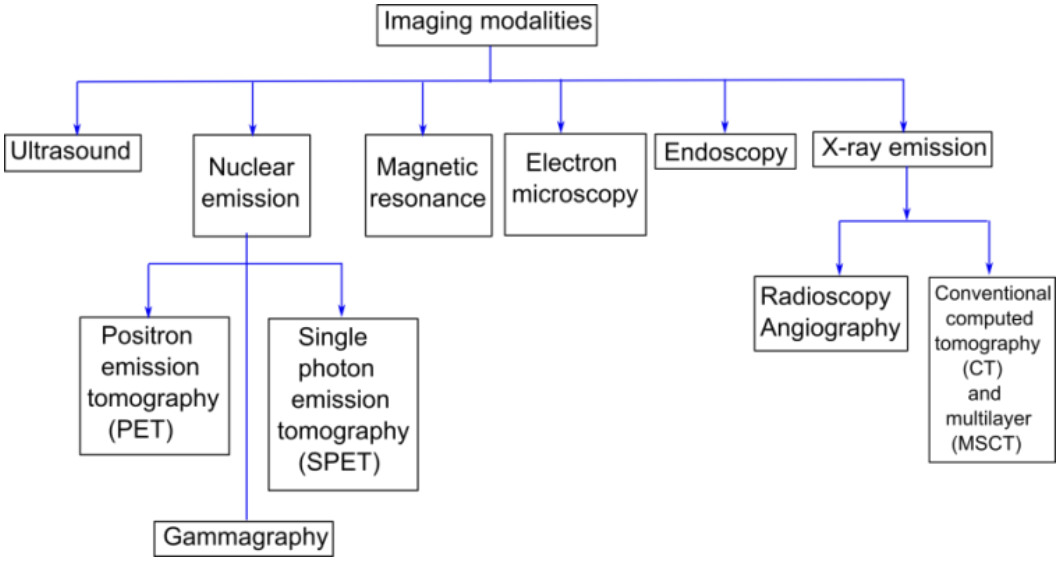

Figure 2. Main imaging modalities used in the medical context.

On the other hand, worldwide, many researchers have developed computational models of brain tumors following approaches such as: deep learning [4,5], random forest algorithm [6], fuzzy logic [7], template system [8], diffusion tensor imaging [9], a BT classification system based on multi-modal image radiomics features [10] and active contour model [11].

In our paper, we focus the attention on the application of a filter bank and level set segmentation technique for semi-automatic segmentation of astrocytomas and meningiomas brain tumors.

2. Materials and methods

2.1. Datasets

Two three-dimensional MRI datasets were used, supplied by the Instituto de BioIngeniería y Diagnóstico S.A., Táchira, Venezuela. They correspond to anatomical structures present in patients with meningioma and astrocytoma tumors.

In addition, BT manual segmentation (ground truth) generated by a neuro-oncologist, is available.

2.2. Computational strategy suggested

Figure 3 shows a scheme of the semi-automatic computational strategy (SACS), proposed in the present investigation, to segment the BT.

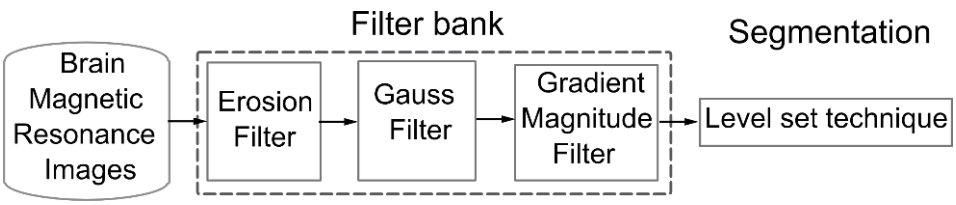

Figure 3. Diagram about the proposed strategy (SACS).

2.3. Filter bank
At this stage, a filter bank is applied to the datasets described in 2.1 section. A brief explanation of these filters is found below.

2.3.1. Erosion filter. The mathematical model of morphological erosion ($\ominus$) filter, considering an image (I) and a structuring element (S), is shown using Equation (1).

$$(I \ominus S) = \{x \,|\, (S)x \subset I\} \tag{1}$$

In this work, a spherical structuring element was considered, and its size is fixed in (3,3,3) according to Ibañez *et al.* [12].

2.3.2. Gaussian Filter. This filter, in several dimensions, is a one-dimensional superposition in the orthogonal directions. This allows the development of implicit discretization schemes of the heat equation with a stable Gaussian filtering process [13]. In this sense, a discrete Gaussian distribution represented by a kernel, with arbitrary size, can be used. The kernel values are obtained according to Newton's binomial theorem. In this paper, during smoothing, to decrease the number of parameters of the Gaussian filter, the size of its neighborhood is arbitrarily set to (3,3,3); while the values of its standard deviation, in any direction, to be equal to the standard deviation of the eroded image generated by the morphological erosion filter.

2.3.3. Gradient Magnitude Filter (GMF). The mathematical model, to obtain a filtered image by gradient magnitude (I_{GM}), is presented by Equation (2). In this work, a scheme based on finite differences was used for GMF computational implementation [14,15].

$$I_{GM} = \left(\left(\frac{\partial I}{\partial i}\right)^2 + \left(\frac{\partial I}{\partial j}\right)^2 + \left(\frac{\partial I}{\partial k}\right)^2\right)^{1/2} \tag{2}$$

where: *i, j, k* represents the spatial directions in which the gradient is calculated and $\left(\frac{\partial I}{\partial i}, \frac{\partial I}{\partial j}, \frac{\partial I}{\partial z}\right)$ are the partial derivatives of the considered image.

2.4. Segmentation
This stage involves two steps: seed point detection and level set segmentation technique. An explanation of these is presented next.

2.4.1. Seed point detection. In each dataset, a neuro-oncologist manually chooses the seed voxel considering the centroid of BT.

2.4.2. Level set technique (LS). This technique allows the iterative deformation of a geometric iso-sphere. The sparse field level set algorithm, based on uniformity of regions (feature image), is chosen to perform the BT segmentation to exploit their ability for both contraction and expansion. The ItkSnap implementation of the sparse field LS algorithm is modeled by the Equation (3) and it is used to perform the brain tumors segmentation [16].

$$I_{LS} = [\alpha G(I) + \beta G(I)\bar{k}]n \tag{3}$$

being: I_{LS} segmented image, α and β LS tuning parameters, $G(I)$ feature image, $\bar{k}$ average curvature of an iso-sphere and n the normal direction in which each point of the iso-sphere moves.

In ItkSnap, the iso-sphere propagation speed is controlled in terms of: a) the feature image (α) and b) the average curvature of the contour being processed (β). The values for α and β can be selected from the real interval [0,1] with step size of 0.1, by default.

During the tuning process, the Jaccard's similarity index (JSI) is used to compare semi-automatic and manual segmentations of BT [17]. The JSI is implemented by Equation (4).

$$\text{JSI} = \frac{|MS \cap SAS|}{|MS \; U \; SAS|} \tag{4}$$

where: MS is the manual segmentation and SAS is the semi-automatic segmentation.

The optimal values for the parameters of the LS (α and β) are matched to the experiment that generates the highest value for the JSI.

3. Results

A maximum JIS of 0.8731 is obtained from the tuning, which generated the optimal parameters for LS technique (α =1, β =0.2).

Figure 4 shows an axial view of an original image using the selected dataset, and the images linked to digital processing developed with the SACS.

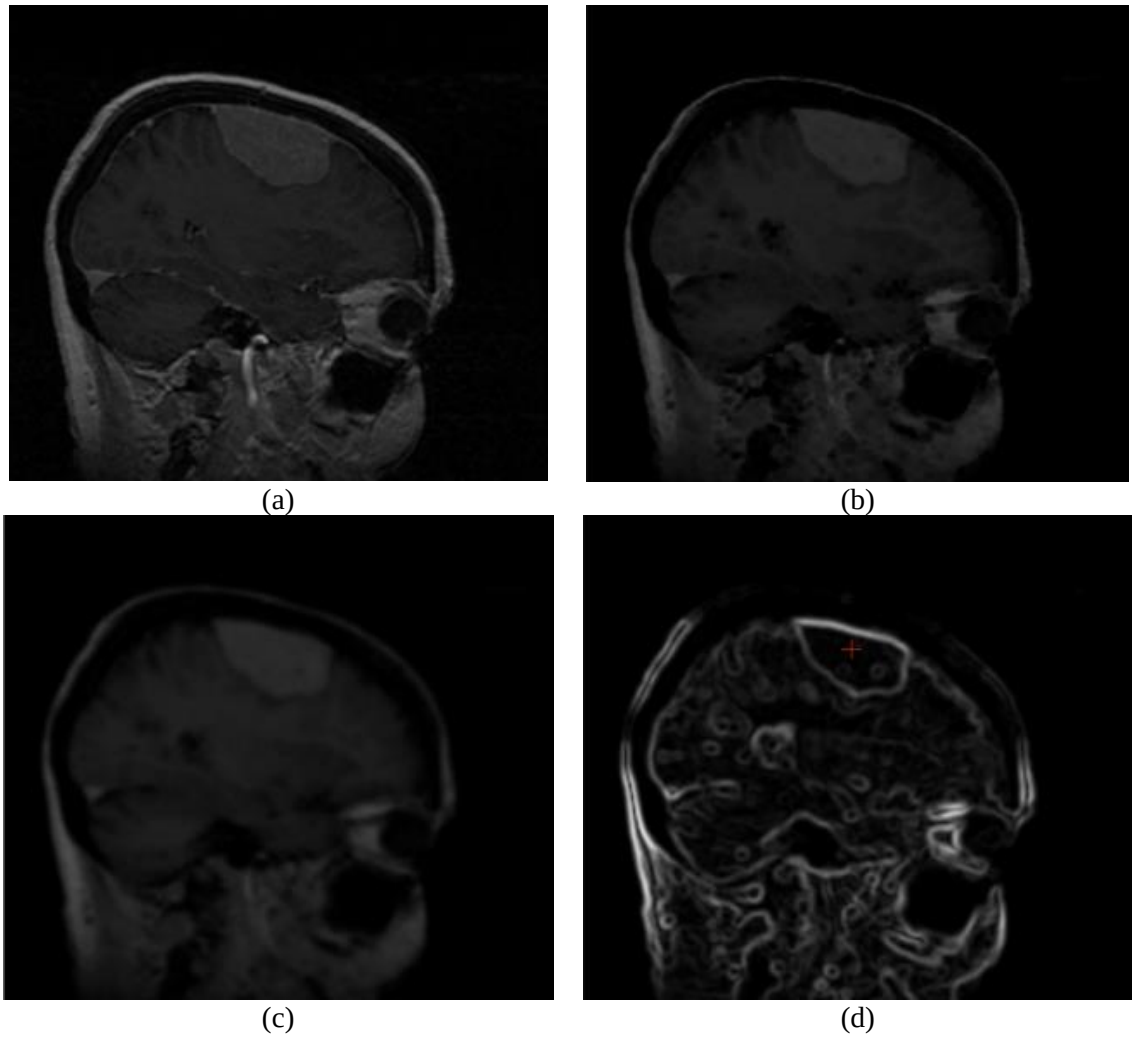

Figure 4. Effect of the SACS using a 2D view of the brain tumor type meningioma. (a) Original, (b) eroded, (c) gaussian, and (d) gradient.

Additionally, Figure 5 shows the three-dimensional morphology of segmented BT.

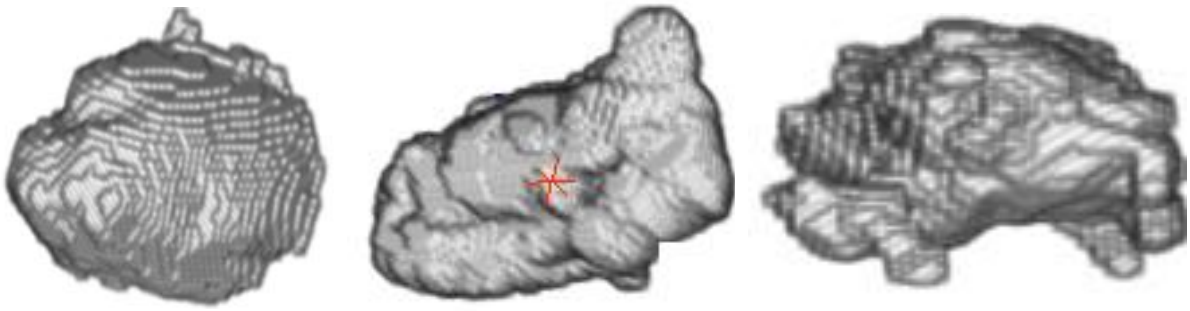

(a) (b) (c)

Figure 5. Three-dimensional representation of segmented brain tumors. (a) Meningioma, (b) astrocytoma type II, and (c) anaplastic astrocytoma type III.

Finally, Table 1 shows the volume values (voxel size multiplied by the number of BT voxels) considering the semi-automatic segmentations of the brain tumors [18].

Table 1. Volumes associated with segmented BT.

BT	Volume(cm^3)
Meningioma	36.8800
Astrocytoma type II	43.5375
Anaplastic astrocytoma type III	24.9500

According to the results, the SACS had a good performance segmenting BT because the maximum JIS value obtained for the BT segmentation was 0.8731. This value is comparable with JSI= 0.8889 [10] and JSI = 0.9470 [9].

Another interesting result is the high morphological variability of considered tumors. This fact contradicts the geometric hypotheses considered by clinical experts, to estimate the BT volume [18].

4. Conclusions

The BT semi-automatic segmentations generated using the proposed strategy, allow the volume calculation of each considered tumor, without any geometrical hypotheses. The JSI value reported in this paper suggests that the SACS have an excellent performance.

It is planned, for the future, to use this strategy in the segmentation and quantification of other types of tumors affecting the human brain, such as multi-form glioblastom, ependymoma, medulloblastoma oligodendroglioma and pituitary tumors.

References

[1] Louis DN, Ohgaki H, Wiestler OD, Cavenee WK 2007 *Classification of tumours of the central nervous system*, 4th edition vol 1 (Lyon: International Agency for Research on Cancer)
[2] Gudbjartsson H and Patz S 1995 The rician distribution of noisy MRI data *Magn. Reson. Med.* **34(1**) 910
[3] Macovski A 1996 Noise in MRI *Magn. Reson. Med.* **36(1)** 494
[4] Casamitjana A, Puch S, Aduriz A and Vilaplana V 2017 3D convolutional neural networks for brain tumor segmentation: A comparison of multi-resolution architectures *Brainlesion: Glioma, Multiple Sclerosis, Stroke and Traumatic Brain Injuries* vol 10154, ed Crimi A, Menze B, Maier O, Reyes M, Winzeck S, Handels H (Berlin: Springer International Publishing) p 150-161
[5] Zhang J, Shen X, Zhuo T and Zhou H 2017 Brain tumor segmentation based on refined fully convolutional neural networks with a hierarchical Dice score *Computer Science* (preprint arXiv:1712.09093)
[6] Kleesiek J, Biller A, Urban G, Kothe U, Bendszus M and Hamprecht F 2014 Ilastik for multi-modal brain tumor segmentation *Proc. MICCAI BraTS Challenge* (Boston: Harvard Medical School) p 12-17
[7] Hsieh T, Liu Y, Liao C, Xiao F, Chiang I and Wong J 2011 Automatic segmentation of meningioma from

non-contrasted brain MRI integrating fuzzy clustering and region growing *BMC Medical Informatics and Decision Making* **11(1)** 11

[8] Kaus M, Warfield S, Nabavi A, Chatzidakis E, Black P and Jolesz F 1999 Segmentation of Meningiomas and low grade Gliomas in MRI vol 1679, ed Taylor C, Colchester A *Medical Image Computing and Computer-Assisted Intervention -MICCAI'99* (Berlin: Springer) p 1-10

[9] Jones T, Bymes T and Yang G 2015 Brain tumor classification using the diffusion tensor image segmentation technique *Neuro-Oncology* **17(3)** 466

[10] Cho H and Park H 2017 Classification of low-grade and high-grade glioma using multi-modal image radiomics features *39th Annual International Conference of the IEEE Engineering in Medicine and Biology Society (EMBC)* (Seogwipo: IEEE) p 3081-3084

[11] Seow P, Win MT, Wong JH, Abdullah NA, Ramli N 2016 Segmentation of solid subregion of high grade gliomas in MRI images based on active contour model (ACM) *Journal of Physics: Conference Series* **694(1)** 012043 1-12

[12] Hans J. Johnson, Matthew M. McCormick, Luis Ibáñez and the Insight Software Consortium 2018 *The ITK Software Guide* Fourth Edition (New York: Kitware Inc.)

[13] Koenderink J 1984 The structure of images *Biol. Cybern.* **50** 363

[14] Pratt W 2007 *Digital image processing* (New York: John Wiley & Sons Inc)

[15] Nadal E, Rupérez Moreno MJ, Martinez-Sanchis S, Monserrat Aranda C, Tur Valiente M and Fuenmayor Fernández FJ 2017 Evaluación basada en el método del gradiente de las propiedades elásticas de tejidos humanos in vivo *Revista UIS Ingenierías* **16(1)** 15

[16] Yushkevich P, Piven J, Cody H, Ho S, Gee J and Gerig G 2005 User-Guided Level Set Segmentation of Anatomical Structures with ITK-SNAP *The Insight Journal* **MICCAI Open-Source Workshop** 1-9

[17] Real R and Vargas J 1996. The probabilistic basis of Jaccard's index of similarity *Sys. Biol.* **45(3)** 380

[18] Hu T, Yan L, Yan P, Wang X and Yue G 2016 Assessment of the ABC/2 method of epidural hematoma volume measurement as compared to computer-assisted planimetric analysis *Biological Research for Nursing* **18** 5